The Impact of CdO on the Radiation Shielding Properties of Zinc-Sodium-Phosphate Glass Containing Barium

A. Saleh[a], R. M. El Shazly[b], H.A. Abd El-Ghany [c,d]

[a] Basic science Department, Higher technological institute, 10th of Ramadan city, Egypt.
[b] Physics Department, Faculty of Science, Al-Azhar University, Cairo, Egypt.
[c] Department of Engineering Mathematics and Physics, Faculty of Engineering (Shoubra), Benha University, Cairo, Egypt.
[d] Faculty of Sciences, Physics Department, Taibah University, Saudi Arabia.

ARTICLE INFO

ABSTRACT

Glass series of chemical composition $40P_2O_5$-$5Na_2O$-$(35–x)ZnO$-$xCdO$-$20BaO$ where, (x = 0, 7.5, 15, 22.5 mol.%) have been prepared by the conventional melt-quenching technique. The shielding characteristics against gamma rays, fast, and slow neutrons have been investigated. The mass attenuation coefficient of the prepared glass samples for gamma rays (μ_m) were determined experimentally at nine energy lines (ranged from 121.8 to 1407.9 keV) emitted from three different γ-rays' radioactive sources. The measured values of (μ_m) were compared with those estimated using MCNP5 code and calculated by WINXCOM software. A good agreement between both experimental and calculated values of μ_m was observed. The half value layers (HVL), mean free path (MFP), effective atomic number (Z_{eff}), effective electron density (N_{el}), and radiation protection efficiency (RPE) were deduced. The results reveal the practicality of using the present glass composition as an effective agent for gamma-rays radioprotection. On the other hand, the macroscopic cross section ($\sum$) of slow neutrons, total slow neutrons, and neutrons with energy > 10 keV at different CdO contents have been determined under good experimental geometric condition. The results indicate a successive improvement of the shielding properties against fast and slow neutrons by increasing CdO concentrations. The effect of CdO addition is clear through the interaction of slow neutrons with cadmium nuclei inside the samples up to 15% which considered optimum CdO percentage in the glass barriers to be used as good neutrons filter.

1. INTRODUCTION

Presently, ionizing radiation is commonly used in numerous areas including medical therapy and diagnostics [1], nuclear power plants, reactor design, space technology applications, nuclear engineering [2], elemental analysis using non-destructive photo-activation analysis (PAA) [3, 4], metal-oxide-semiconductors (MOS) capacitor irradiation response test [5, 6], food treatment [7], archaeology (carbon dating) and security devices [8] etc. Long time exposure to radiation causes significant tissues damage including cancer, radiation infections, mutation, and sometimes even death. At genetic level, radiations further impact the future of living organ systems [9]. From this perspective, it is required to continue providing shielding materials to minimize exposure to radiation in areas where people are expected to receive ionizing radiation.

Almost every substance can be used to protect harmful radiation if this substance has sufficient thickness to absorb the radiation to a fair extent [10]. Commonly, different types of concretes are used to protect from harmful radiations [8]. There are many disadvantages of concrete such as destructive effects in its structure due to loss of water contained in it over the time of use and it's fully not transparence to visible light and thus it is impossible to look through a concrete radiation shield [11]. Because of their low cost, visible light transparence ability and easily to shape, glasses have increasingly studied by many researchers as promising radiation shielding materials [12].

Several studies have been performed on various glass systems to investigate their ability to attenuate different nuclear radiation. Most of these studies use lead as a former in these glassy structures. But due to its toxicity and high cost, lead however, may not be the optimum glassy former in the glass composition [13]. Already many studies to develop a new type of transparent glassy systems to enhance shielding properties have been devoted [14 -19]. As the ordinary window sand glasses based on silica and smaller amounts of alkalis oxides (Na_2O or K_2O) to reduce high melting point, many of the developed radiation shielding glasses are SiO_2–PbO based. However, phosphate glasses are attractive for the design of many optical systems compared to other glass systems as the absorption edge of phosphate glasses is strongly shifted toward the short- wavelength range (next to UV range) making it more transparent for visible light [20].

Among other oxide glasses (borate, silicate, etc.), phosphate glasses have many unique advantages such as, ability to retain amorphous, it can handle high-concentration of transition metal ions [21, 22], unique chemical and physical structural and compositional capabilities that simplify modification of physical behavior and chemical substance [23]. Therefore, one or more multivalent oxides (ZnO, Al_2O_3, SnO, PbO, Fe_2O_3, etc.), should be doped to develop the glass performance. These additions of such oxides help the development of the following chemical bonds (Zn-O-P, Al-O-P, Fe-O-P, Sn-O-P, Pb-O-P) and thus greatly increase their chemical stability [24]. In the present work ZnO was added. In addition, Ba-based glasses possess strong absorption for x-ray and gamma-rays and non-toxicity compared with lead- and bismuth-based glasses [25]. Moreover, it has property to improve the rigidity of glass material [26].

From point of interest, CdO comes as a divalent metal oxide which can be featured with two different oxidation states. Because of its large atomic number, high density, low binding energy, CdO is considered here as an important oxide for different kinds radiation shielding applications. According to Osman AĞAR [27], addition of CdO as a network modifier enhances the shielding properties of tellurite-based glasses. Recently, the effect of adding CdO on the mechanical and radiation shielding properties of sodium borate glasses have been investigated [15].

Generally, In contrast to utilization of traditional shielding materials such as concrete, lead (Pb), there is a continues need to obtain more glass compositions having some advantages such as: (i) possibility of transportation from one place to another, (ii) transparent materials that can be used in various technological applications such as iodine injection radiotherapy room. However, literature review showed that no study has been done on the radiation shielding properties of cadmium doped phosphate glasses. This has encouraged us to apply a broad-range investigation on the radiation shielding performance of different types of cadmium doped phosphate glass as a new member of the radiation shielding family.

The present work is devoted to study the effect of CdO on the shielding properties of zinc sodium phosphate glass containing barium. Hence, glass series of chemical composition $40P_2O_5$-$5Na_2O$-$(35–x)$ZnO-xCdO-20BaO where, ($x = 0$, 7.5, 15, 22.5 mol.%) have been prepared. So, the role of CdO shall be discussed for enhancing the shielding properties of the prepared glass against gamma rays, fast and slow neutrons in order to be used as a neutrons filter.

## 2. Experimental and theoretical aspects

2.1 Samples preparation:

Glasses in the $40P_2O_5$-$5Na_2O$-$(35-x)$ZnO-xCdO-20BaO (x= 0, 7.5, 15, 22.5 mol %) system have been prepared by the melt quenching method using high purity chemicals. After weighing and thoroughly mixing, batches of 90 g in weight were grinded in a mortar pestle for 30 minutes. The mixtures were heated for 30 minutes in a muffle furnace regulated at 260±5 °C to release the gases such as CO_2 and NH_3. Then the batches were melted in a platinum crucible with a closed lid at 1000±5 °C for 45 min. Vitreous samples were obtained by pouring the melt into pre-heated stainless-steel molds. The samples then were annealed near the glass transition temperature for 2 hours to remove internal stresses. Finally, the glasses were cut, ground and polished to obtain samples with plan-parallel surfaces with dimensions (4 cm × 4 cm) having an average thickness of 6 mm for further radiation shielding measurements. Density measurements of the synthesized glasses were achieved at room temperature using Archimedes' principle with toluene as an immersion liquid. a digital balance of sensitivity 10^{-4} g was used, and density values were obtained by three repeated measurements with an error of ±0.05%. The chemical composition (mole fraction) and density of prepared glass samples are listed in Table 1.

Table (1): Chemical composition (mole fraction) and density of prepared glass samples.

Sample	Mole fraction					Density (g/cm³)
	P_2O_5	ZnO	Na_2O	CdO	BaO	
S1	0.4	0.35	0.05	—	0.2	3.015
S2	0.4	0.275	0.05	0.075	0.2	3.349
S3	0.4	0.200	0.05	0.150	0.2	3.458
S4	0.4	0.125	0.05	0.225	0.2	3.498

2.2 *Gamma ray measurements:*

The gamma ray attenuation coefficients of the prepared glass samples were obtained at nine energy lines using collimated beam of γ-rays emitted from 3.7 μCi Eu-152, 9.5 μCi Cs-137, and 4.9 μCi Co-60 radioactive sources. Figure (1) shows the schematic diagram of gamma ray detection system, where a 3″ x 3″ NaI (Tl) scintillation detector was used to measure the gamma ray intensities for the studied energy lines.
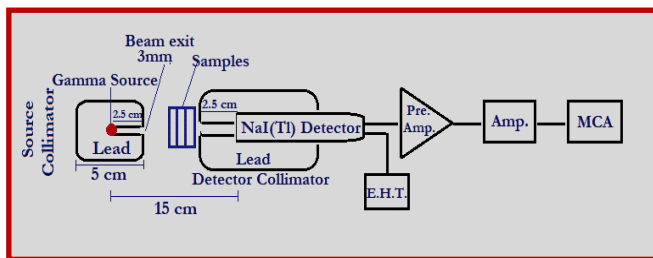
Fig. (1): Schematic diagram of gamma ray detection setup.

The capability of any absorber to attenuate the photons of certain energies can be estimated using the mass attenuation coefficient, μ_m (cm²/g) given by the Beer-Lambert's equation [28]:

$$\mu_m = -\frac{ln(\frac{I_0}{I})}{x\rho} \tag{1}$$

where I_0 and I are the incident and the transmitted intensities, ρ (g/cm³) is the density of the material and x (cm) is the thickness of the absorber.

The result values of μ_m were compared by calculated values for a mixture of different elements by "WinXCom" computer program (version 3.1) [29]. And also, with that estimated by MCNP5 code.

$$\mu_m = \Sigma_i^n W_i \left(\frac{\mu_i}{\rho_i}\right) \tag{2}$$

where, $\left(\frac{\mu_i}{\rho_i}\right)$ is the mass attenuation coefficient for the individual element in each mixture sample, while W_i is

the fractional weight of the element in each mixture sample.

The mean free path, λ (cm), the half value layer HVL (cm), and tenth value layer TVL (cm) of each sample concentration and total gamma rays, are characterize the effectiveness of gamma-ray shielding, were determined using the following equations [28]:

$$\lambda = \frac{1}{\mu}, \qquad HVL = \frac{\ln(2)}{\mu}, \qquad TVL = \frac{\ln(10)}{\mu} \tag{3}$$

where μ (cm⁻¹) is the linear attenuation coefficient for the material under consideration.

The effective atomic number Z_{eff} (dimensionless quantity) can be calculated by [28]:

$$Z_{eff} = \frac{\sigma_{t,a}}{\sigma_{t,el}} = \frac{\sum_i n_i A_i (\mu/\rho)_i}{\sum_i n_i A_i / Z_i (\mu/\rho)_i} \tag{4}$$

Electron density, N_{el} (number of electron per gram) of the material can be derived using μ_m and $\sigma_{t,a}$. [30]:

$$N_{el} = \frac{\mu_m}{\sigma_e} = \frac{Z_{eff} N_A \sum_i n_i}{M} \tag{5}$$

The radiation protection efficiency of a shielding material is defined as [31]:

$$RP = \left(1 - \frac{I}{I_0}\right) \times 100 \tag{6}$$

2.3 *Neutron measurements:*

The Boron tri-fluoride (BF_3) neutron detector was used to detect a collimated slow neutrons, total slow neutrons (primary slow as well as slowdown in the studied glass samples), and neutrons with energy greater than 10 keV beam emitted from ^{241}Am-Be neutron source with activity 3.7 GBq. The neutron transmitted fluxes were measured to deduce the values of macroscopic neutron cross-section ($\sum$) according to equation (7) [32]. In case of slow neutrons measurements, the collimated beam was slowed down by 7 cm polyethylene block behind the sample, also the neutron of energy below 10 keV was cut off by a block of Born carbide B_4C. The Schematic diagram of experimental setup was shown in Fig. 2.

$$I_n = I_o e^{-\Sigma x} \tag{7}$$

Where Σ is the neutron macroscopic cross section (cm⁻¹), I_n and I_o are the neutron fluxes after and before transmitted through the sample barriers respectively, and x is the sample thickness.
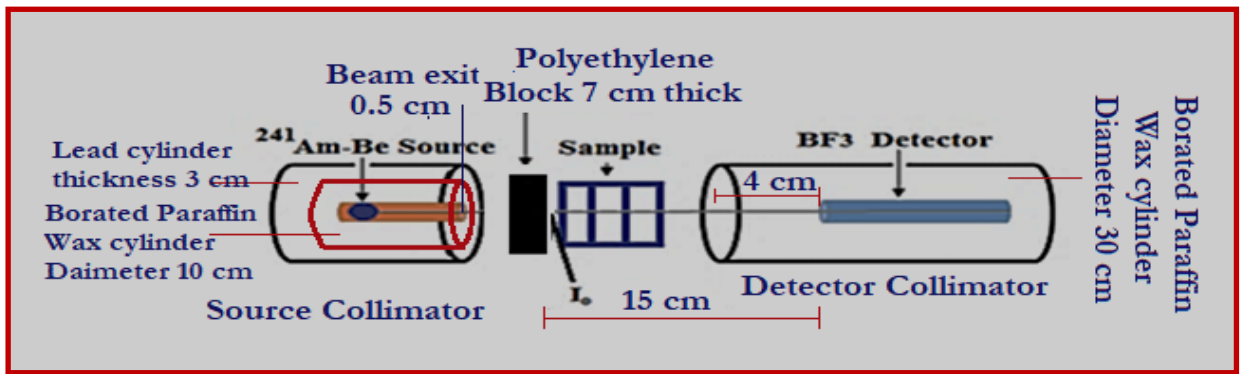
Fig. (2): Schematic diagram of Neutron detection setup.

The maximum experimental errors in attenuation coefficients and half value layers for both gamma-ray and neutron attenuation measurements were evaluated using the following error formulas [33].

$$\Delta\sigma = \frac{1}{x\rho}\sqrt{\left(\frac{\Delta I_0}{I_0}\right)^2 + \left(\frac{\Delta I_{(\gamma)}}{I_{(\gamma)}}\right)^2 + \left(\frac{\Delta x\rho}{x\rho}\right)^2\left(ln\left(\frac{I_0}{I_{(\gamma)}}\right)\right)^2} \qquad (8)$$

$$(\Delta HVL) = (HVL)\sqrt{\left(\frac{\Delta\mu}{\mu}\right)^2 (ln2)^2} \qquad (9)$$

$$\Delta\Sigma = \frac{1}{x}\sqrt{\left(\frac{\Delta I_0}{I_0}\right)^2 + \left(\frac{\Delta I_{(n)}}{I_{(n)}}\right)^2 + \left(\frac{\Delta x}{x}\right)^2\left(ln\left(\frac{I_0}{I_{(n)}}\right)\right)^2} \qquad (10)$$

$$(\Delta MFP) = (MFP)\sqrt{\left(\frac{\Delta\Sigma}{\Sigma}\right)^2} \qquad (11)$$

3. RESULTS AND DISCUSSION

3.1 X-ray diffraction studies

X-ray diffraction (XRD) technique was employed to check the glass formability of the obtained samples. Fig. 3 shows the XRD patterns of the prepared samples with different concentrations of CdO. The results show diffused scattering with no Bragg's peaks can be observed. This confirms the amorphous nature of the prepared samples. One can observe a broad profile around $2\theta = 20^o$ which suggest the existence of some short-range order in the glass samples.
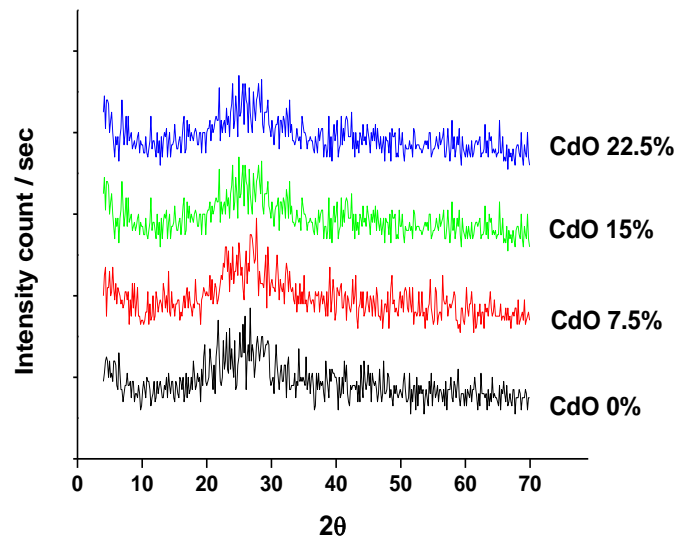

Fig. (3): XRD patterns of glass samples for different CdO content.

3.2 Gamma-rays attenuation coefficients

The attenuation coefficient (μ_m) for the present glass samples have been determined at nine energy lines of gamma-rays (121.78, 344.27, 661.64, 778.9, 964, 1112.4, 1173.23, 1332.51, and 1407.92 keV). Different thicknesses of the glass barriers have been applied at each concentration of CdO (varying from 0 - 1.7 cm).The measured γ-rays intensities transmitted through glass samples were given as a function of superficial densities ρ_x (g/cm³) of glass barriers. The average values of the total mass attenuation coefficients μ_m (cm²/g) of the present glass samples were deduced using the slope of the attenuation curves. The measured values of mass attenuation coefficient (μ_m) for the glass samples at different cadmium concentration have been compared with those estimated using MCNP5 code and those calculated using WINXCOM software and listed in table2. A quick look into the results in table 2 show a good agreement between the experimental values of
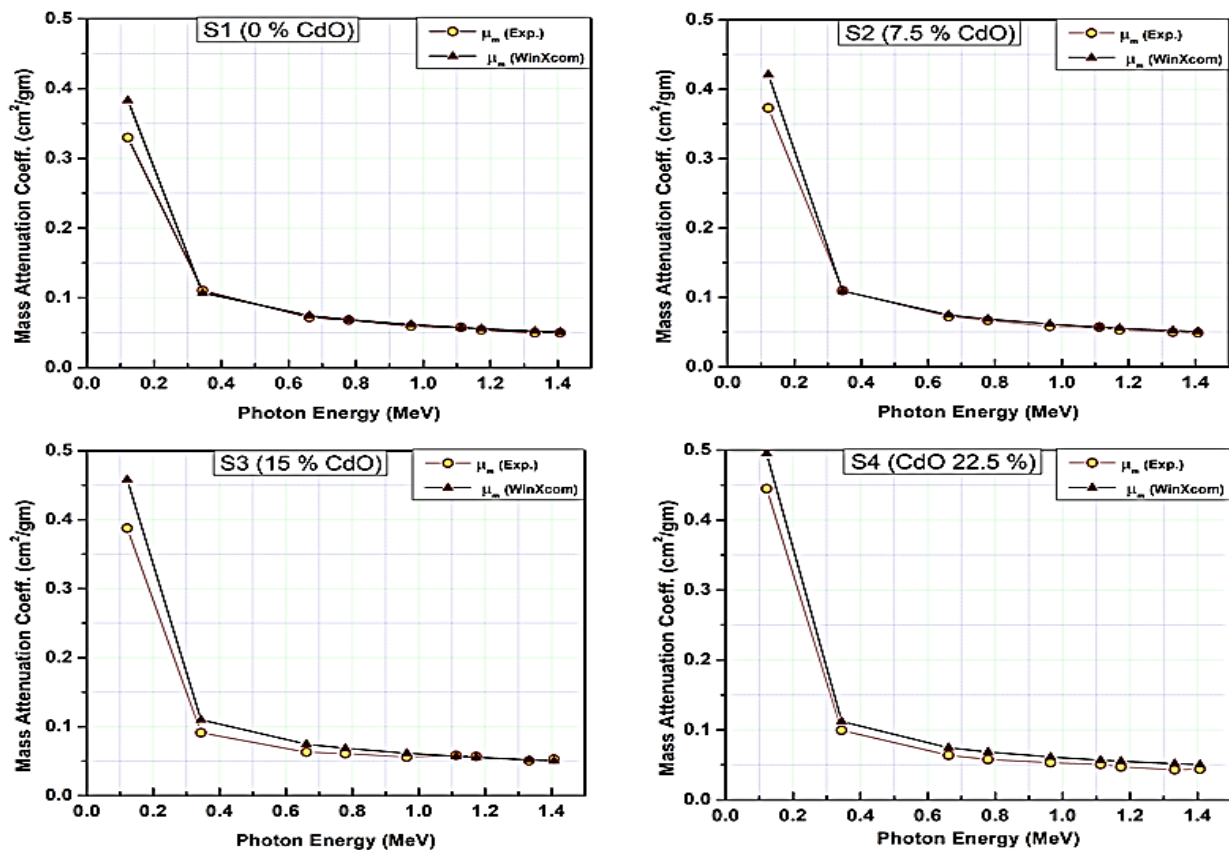
the mass attenuation coefficient and the corresponding theoretical data calculated using WINXCOM program (version 3.1) and that estimated using MCNP5 code. However, the experimental values of the mass attenuation coefficient are found to be slightly lowered than those theoretically obtained from WINXCOM and MCNP5. This may be attributed to the crystalline nature of the molecular arrangement of detector source which can make incident beam geometry narrow, possibly reducing the μ_m values[19].

Table (2): The experimentally measured mass attenuation coefficients (cm^2/g) along with that estimated theoretically for the selected glasses.

Energy (keV)	S1			S2			S3			S4		
	WinX	Exp.	MCNP5	WinX.	Exp.	MCNP5	WinX.	Exp.	MCNP5	WinX.	Exp.	MCNP5
121.78	0.383	0.3296 ± 0.014	0.3841	0.421	0.3729 ± 0.004	0.4217	0.458	0.3877 ± 0.003	0.4589	0.495	0.4448 ± 0.004	0.4920
344.27	0.107	0.1104 ± 0.016	0.1081	0.109	0.1094 ± 0.009	0.1100	0.110	0.0911 ± 0.003	0.1111	0.112	0.0993 ± 0.005	0.1117
661.64	0.075	0.0718 ± 0.004	0.0749	0.075	0.0722 ± 0.003	0.0753	0.075	0.0631 ± 0.002	0.0755	0.075	0.0638 ± 0.002	0.0752
778.90	0.068	0.0682 ± 0.003	0.0691	0.069	0.0668 ± 0.001	0.0694	0.069	0.0609 ± 0.001	0.0683	0.068	0.0577 ± 0.002	0.0681
964.00	0.062	0.0594 ± 0.007	0.0629	0.062	0.0579 ± 0.005	0.0617	0.062	0.0558 ± 0.004	0.0621	0.061	0.0532 ± 0.006	0.0621
1112.4	0.057	0.0576 ± 0.001	0.0587	0.057	0.0569 ± 0.001	0.0581	0.057	0.0583 ± 0.001	0.0580	0.057	0.0507 ± 0.001	0.0579
1173.2	0.055	0.0540 ± 0.001	0.0561	0.056	0.0529 ± 0.001	0.0561	0.056	0.0568 ± 0.002	0.0560	0.055	0.0470 ± 0.001	0.0556
1333.5	0.052	0.0499 ± 0.001	0.0529	0.052	0.0498 ± 0.001	0.0528	0.052	0.0503 ± 0.001	0.0526	0.052	0.0431 ± 0.001	0.0528
1407.9	0.050	0.0497 ± 0.001	0.0514	0.051	0.0487 ± 0.003	0.0520	0.051	0.0529 ± 0.001	0.0517	0.051	0.0439 ± 0.001	0.0515

The energy dependence of the mass attenuation coefficient (μ_{exp} and $\mu_{WINXCOM}$) for different cadmium concentrations is depicted in Fig. 4.

Fig. (4): Mass attenuation coefficient of the glass samples as a function of gamma ray energy.

In general, both μ_{exp} and $\mu_{WINXCOM}$ follow one common trend for all glass samples where it decreases by increasing the photon energy. It is quite clear that at low photon energies (between 121 and 344 keV), the mass attenuation coefficient is found to be decreased dramatically with increasing the photon energy. This may be explained on the basis that the prominent reaction here is the photoelectric absorption (PE) mechanism [34]. Meanwhile in region from 344 keV up to 1407 keV, a slight decrease in mass attenuation coefficient can be observed as the gamma-ray energy increases. Such behavior of the mass attenuation coefficient in this energy interval can be ascribed to the preeminence of Compton scattering process [35].

Fig. 5 shows the measured values of mass attenuation coefficient (μ_m) for glass samples at different energies. It can be indicated that the mass attenuation coefficient for the present glass system is enhanced by increasing CdO content.
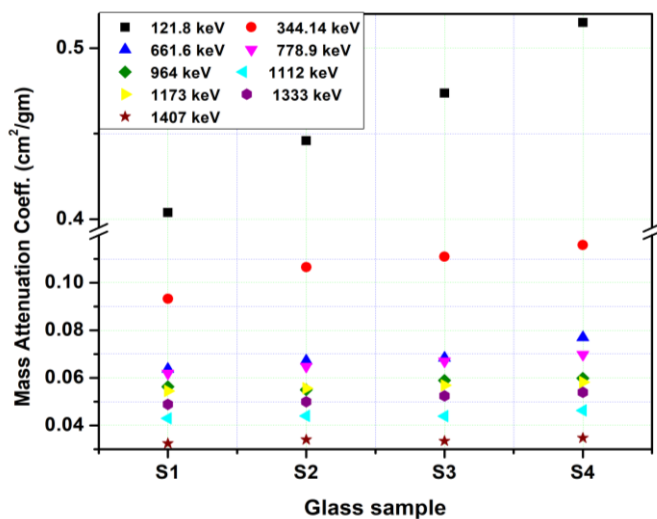

Fig. (5): The measured values of mass attenuation coefficient (μ_m) for the glass samples at different energies.

The obtained results of μ/ρ were used to calculate the mean free path of prepared samples using eq.(3) and graphically introduced in Fig.6. It was observed that the values of MFP were reduced with the increase in CdO concentration as well as the density of glass samples (as can be seen in Table 1). From Fig.6, the MFP of glass sample (S4) possesses the lowest values. This indicates that, the radiation shielding performances of the present glasses are improved with the addition of CdO modifier.
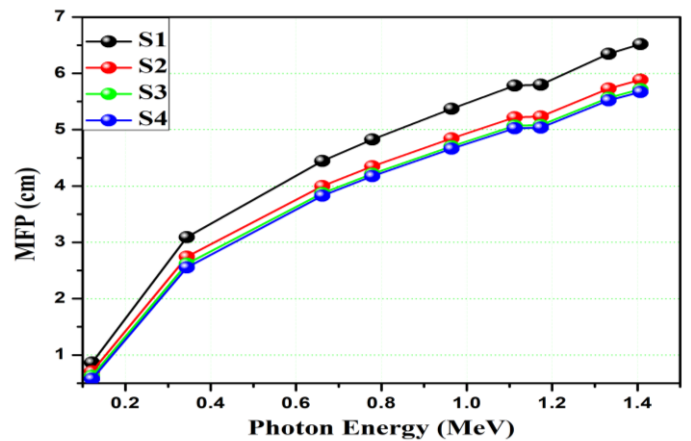

Fig. (6): Variation of mean free path with photon energy between 0.015 and 10 MeV.

The half value layer (HVL) for the present glass barrier samples is determined using equation (3). Table 3 shows the calculated values of HVL for the nine gamma-ray energies at different CdO concentrations. The obtained data reveal a general decrease in HVL for all energy lines by increasing content of CdO. The percentage of decrement in HVL is found to be ranged from 50% (for 121.8keV) to 15% (for 1407 KeV). In other words, HVL decreases more effectively for lower photon energies than for higher photon energies with increasing concentrations of CdO from 0% up to 22.5%.

Table (3): Half value layer (HVL) for all samples.

Energy (keV)	HVL (cm)				(HVL_{S1}-HVL_{S4}/HVL_{S1})
	S1	S2	S3	S4	100(%)
121.78	0.5985	0.4911	0.4370	0.3995	49.8244
344.27	2.1419	1.9013	1.8160	1.7708	20.9601
661.64	3.0801	2.7723	2.6842	2.6529	16.1070
778.90	3.3448	3.0142	2.9221	2.8914	15.6820
964.00	3.7226	3.3589	3.2603	3.2302	15.2458
1112.40	4.0076	3.6178	3.5134	3.4827	15.0734
1173.23	4.0181	3.6269	3.5219	3.4908	15.1076
1333.51	4.3981	3.9712	3.8574	3.8246	14.9955
1407.92	4.5179	4.0797	3.9630	3.9295	14.9749

The measured values of the mass attenuation coefficient have been utilized to evaluate the effective atomic number (Z_{eff}) and electronic density (N_{el}) for the present glass samples using Eqs. (4 & 5) respectively. Figs. 7 and fig. 8 show that the variations of the calculated values of Z_{eff} and N_{el} as a function of γ-ray energies. It's clear that they have the same trend for all glass samples studied.
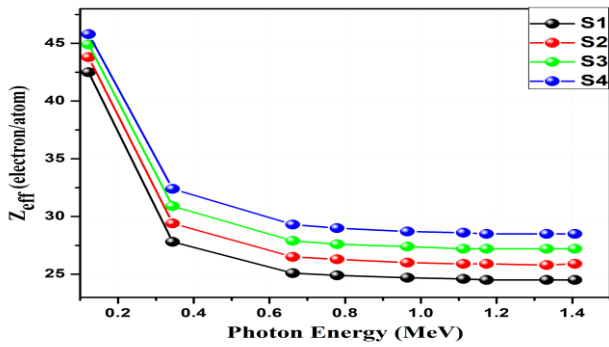

Fig. (7): Variation of Z_{eff} with photon energy for all selected glass samples
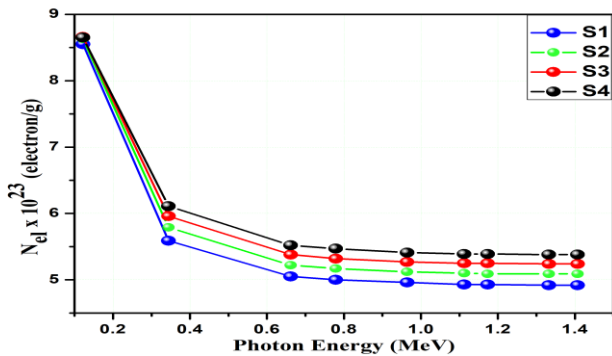

Fig. (8): Variation of N_{el} with photon energy for all selected glass samples

In addition, figs. 7 and fig. 8 show that, the values of Z_{eff} and N_{el} were decreased for all glass samples with increasing the photon energy up to 0.356 MeV (the photoelectric effect is dominant at low energies and hence Z_{eff} is described by this process for the photon absorption). After that, they seem to be constant due to Compton scattering's linear Z dependency (Compton scattering is the most powerful process at this energy region). Here, both Compton scattering and pair production will be the main processes in comparison with photoelectric effect process and this can affect the photon absorption by Z_{eff}.

It is very clear that for the prepared glass samples, the calculated values of Z_{eff} and N_{el} are improved by

increasing the content of CdO. As previously discussed, this can be due to changes in the mass attenuation coefficient. On the other hand, Fig. 9 reveals a strong correlation between Z_{eff} and N_{el} derived from the deduced values which verified the closely related photon energy dependence of Z_{eff} and N_{el}.
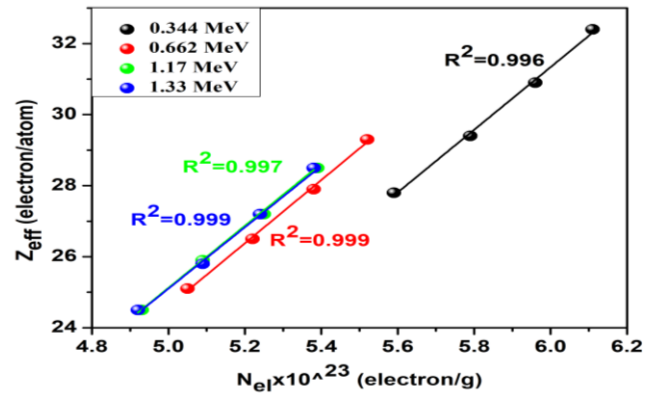

Fig. (9): Correlation between effective atomic number (Z_{eff}) and electron density (N_{el}) of glass samples for experimental results at 0.356, 0.662, 1.173 and 1.33 MeV.

The variation of the RPE (radiation protection coefficient) as a function of photon energies for the present glasses have been determined and enlisted in Table. 4. The obtained data indicate that RPE reduces from its maximum value at 121 keV with increasing the photon energy for all prepared glass samples. It can be clearly observed that the attenuation capability of gamma photons is increased by increasing CdO concentrations from 0% up to 22.5%. The results reveal the practicality of using the present glass composition as an effective agent for gamma-rays shielding.

Table (4): Variation of experimentally measured RPE for the selected glasses with photon energy.

Energy (keV)	RPE (%)			
	S1	S2	S3	S4
121.78	96.899	98.549	99.142	99.451
344.27	62.115	66.494	68.172	69.089
661.64	49.083	52.760	53.908	54.328
778.90	46.289	49.829	50.909	51.277
964.00	42.792	46.149	47.148	47.461
1112.40	40.474	43.710	44.664	44.951
1173.23	40.394	43.629	44.584	44.875
1333.51	37.669	40.757	41.665	41.934
1407.92	36.882	39.926	40.821	41.085

3.3 Neutron measurements and calculations.

The measured neutron intensities transmitted through glass samples were given as a function of glass thickness (attenuation curves).The slope of these curves has been used to determine the values of macroscopic cross-sections of slow neutrons, total slow neutrons and neutrons of energy > 10keV in the investigated glass samples. Fig.10 shows the variation of such values of the macroscopic cross-section with increasing concentrations of CdO in the samples. It can be observed that in case of slow and total slow neutrons, the values of macroscopic cross-section is increased by increasing content of CdO from 0% up to 15% and there is no significant increase in that values by increasing the concentration of CdO content above 15 %. In case of neutrons of energy > 10keV, the values of macroscopic cross-section seem to be nearly constant by addition CdO to glass samples from 0 up to 22.5 %. Also, the data indicate that, the experimental values of $\sum$ for slow neutrons are the highest value from the others after addition of CdO in the samples. This can be explained by the highest probable interaction is a captured of slow neutron by the Cd added in glass samples; (n, γ) reactions, where the cross-section value of slow neutron with natural cadmium is about 2918 barn [43]. While for total slow neutrons there is a competition between two process in this range of neutron energies which considered slow down neutron energy due to inelastic scattering, i.e. (n, n) reactions for fast neutrons by the barium nuclei, and the cut-off neutron with energy less than 0.4 eV by cadmium nuclei. But in the case of neutron with energies > 10 keV there is no effect of cadmium nuclei on these similar neutron energies, so we found that there is no significant changes of the value of macroscopic cross-section by increasing the concentration of cadmium nuclei in glass sample, and Interaction values are attributed to inelastic scattering for neutrons by barium nuclei only.
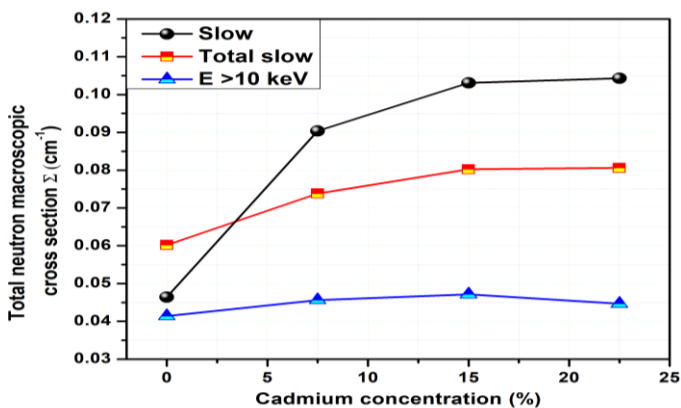

Fig. (10): Variation of total neutron, emitted from 241Am-Be source, macroscopic cross-section with Cd concentration in glass samples.

Fig. 11 shows the variation of the total neutron cross-section with neutron energy for cadmium and zinc as estimated using MCNP5 code. It can be easily observed that cadmium have a total neutron cross-section larger than that of zinc especially in the low energy range.
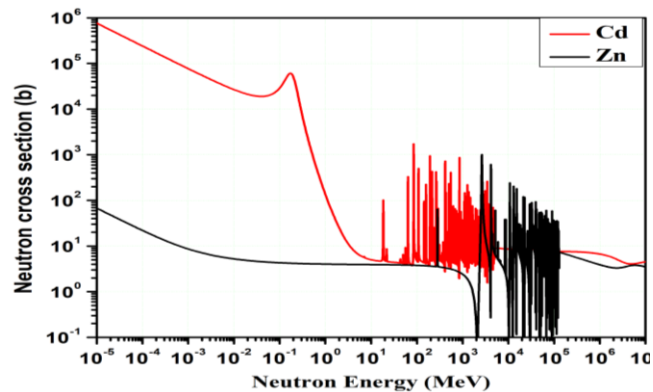

Fig. (11): Variation of total neutron cross-section with neutron energy of Cd and Zn.

In addition, some important parameters of neutron attenuation have been determined like half value layer (HVL) and mean free path (λ). The results for such parameters at different neutron energies are listed in Tables 5 and 6 respectively. The obtained data indicate a successive improvement in the attenuation properties of neutrons by increasing concentrations of CdO. The results reveal the effectiveness of using the present glass composition in the various applications of neutron shielding.

Table (5): The neutrons half value layers for glass samples under investigation

Neutron Energy	HVL (cm)				(HVL$_{S1}$-HVL$_{S4\%}$/HVL$_{S1}$) 100(%)
	S1	**S2**	**S3**	**S4**	
Slow	14.93	7.671	6.724	6.646	55.8
Total slow	11.516	9.389	8.639	8.599	25.9
E> 10 keV	16.746	15.194	14.704	15.526	7. 6

Table (6): The neutrons mean free paths for glass samples under investigation

Neutron Energy	MFP (λ-cm)			
	S1	**S2**	**S3**	**S4**
Slow	21.541	11.066	9.7010	9.5870
Total slow	16.613	13.545	12.465	12.406
E >10 keV	24.160	21.920	21.214	22.399

3.4. Macroscopic effective removal cross section for fast Neutrons Σ_R

The macroscopic effective removal cross section (Σ_R) is the probability of a neutron undergoing certain reaction per unit length of moving through the shielding material [36]. The Σ_R values for the present glass samples have been evaluated at 2 MeV using MCNP5 code and the results are listed in Table 7. The calculated values of Σ_R are varied in the range (0.0813–0.091 cm^{-1}). However, the sample S3 is found to have the highest value of Σ_R. This supports the suggestion that the sample S3 is more effective for fast neutron attenuation than the other samples in the present glass composition.

Table (7): Fast neutrons effective removal cross sections for CdO containing glasses.

Sample	Σ_R (cm^{-1})
S1	0.0813
S2	0.0890
S3	0.0910
S4	0.0900

CONCLUSIONS

In the present work successful glass series of chemical composition 40P$_2$O$_5$-5Na$_2$O-(35–x)ZnO-xCdO-20BaO where, (x = 0, 7.5, 15, 22.5 mol.%) have been prepared in order to study their shielding characteristics against gamma rays, fast and slow neutrons. The attenuation coefficient (μ_m) of the present glass samples have been determined at nine energies of gamma-rays (121.78, 344.27, 661.64, 778.9, 964, 1112.4, 1173.23, 1332.51, 1407.92 keV). For all glass samples, μ_m is found to be decreased by increasing the photon energy. At low photon energies (between 121.8 and 344.14 KeV), μ_m is decreased dramatically with increasing the photon energy which is attributed to the photoelectric absorption mechanism meanwhile in region from 344.14 keV up to 1407 keV, μ_m exhibits a slight decrease which is ascribed to the preeminence of Compton scattering process. The measured values of mass attenuation coefficient for the glass samples at different cadmium concentration are observed to be greatly consistent with those estimated using MCNP5 code and calculated theoretically using WINXCOM software. The half value layers (HVL), mean free path (MFP), effective atomic number (Z$_{eff}$), effective electron density (N$_{el}$), and radiation protection efficiency (RPE) have been reported. The role of increasing CdO is clear and the results reveal the practicality of using the present glass

composition as an effective agent for gamma-rays radioprotection.

On the other hand, the macroscopic cross-sections (Σ_n) of the prepared glass samples against slow, total slow and neutrons with energy > 10 keV have been determined under good experimental geometric condition. In case of total slow and slow neutrons, Σ_n is increased by increasing content of CdO from 0% up to 22.5% with no significant change between CdO concentrations from 15 % to 22.5%. In case of neutrons of energy > 10 keV, Σ_n is increased by increasing CdO concentration from 0% to 15% then it decreases as CdO concentration increases to 22.5%. The half value layer (HVL) and relaxation length (λ) are also calculated. The macroscopic effective removal cross section (Σ_R) for the present glass samples have been evaluated at 2 MeV using MCNP5 code. The calculated values of Σ_R are varied in the range (0.0813–0.091 cm^{-1}). The data indicate general improvement in the shielding properties of neutrons by increasing concentrations of CdO with the sample of 15% cadmium concentration is the optimum percentage in glass barriers, and it is possible to be used as a good neutrons filter. The data obtained in this study should be helpful in potential applications.

REFERENCE

[1] Parminder Kaur, K.J. Singh, Murat Kurudirek, Sonika Thakur, 2019, Study of environment friendly bismuth incorporated lithium borate glass system for structural, gamma-ray and fast neutron shielding properties, Spectrochimica Acta Part A: Molecular and Biomolecular Spectroscopy, 223, 117309

[2] Murat Kurudirek, 2017Matori, K.A., Sayyed, M.I., Sidek, H.A.A., Zaid, M.H.M., Singh, V.P., 2017. J. Non-Cryst. Solids 457, P.97..

[3] Agar, O. Boztosun, I. Segebade, C., 2017. Multi elemental analysis of some soils in Karaman by PAA using a cLINAC. Appl. Radiat. Isot., 122, P.57–62.

[4] Kavun Y, Boztosun I, Dapo H, MaraşI, Segebade C., 2018. Determination of the Sr/Ca ratio of tooth samples by photo activation analysis in Southern Turkey. Radio. Chim. Acta.

[5] Kahraman A, Yilmaz E, Aktag A, Kaya S., 2016. Evaluation of radiation sensor aspects of Er2O3 MOS capacitors under zero gate bias. IEEE Trans Nucl. Sci., 63. P.1284–93.

[6] Kahraman A, Yilmaz E., 2017. Irradiation response of radio-frequency sputtered Al/ Gd2O3/p-Si MOS capacitors. Radiat. Phys. Chem., 139, P.114–9.

[7] Wang XB, Wang CN, Zhang YC, Liu TT, Lv JP, Shen X, 2018. Effects of gamma radiation on microbial, physicochemical, and structural properties of whey protein model system. J. Dairy Sci.

[8] Dong M. G. , Sayyed M. I., Lakshminarayana G.,∗ , Çelikbilek Ersundu M., Ersundu A.E., Priyanka Nayar, Mahdi M.A., 2017, Investigation of gamma radiation shielding properties of lithium zinc bismuth borate glasses using XCOM program and MCNP5 code, Journal of Non-Crystalline Solids, 468 p 12-16

[9] Obaid SS, Gaikwad DK, Pawar PP., 2018. Determination of gamma ray shielding parameters of rocks and concrete. Radiat. Phys. Chem., 144, P.356–360.

[10] Tuscharoen, S. Kaewkhao, J. Limkitjaroenporn, P. Limsuwan, P. Chewpraditkul, W., 2012. Improvement of BaO: B2O3: Fly ash glasses: radiation shielding, physical and optical properties, Ann. Nucl. Energy 49, P.109-113,

[11] Ashok Kumar, Sayyed M.I., Mengge Dong, Xiangxin Xue, Effect of PbO on the shielding behavior of ZnO–P2O5 glass system using Monte Carlo simulation, 2018, journal of Non-Crystalline Solids, 481, pp. 604-607

[12] Ashok Kumar, Sayyed M.I., Mengge Dong, Xiangxin Xue, 2018, Effect of PbO on the shielding behavior of ZnO–P2O5 glass system using Monte Carlo simulation, journal of Non-Crystalline Solids, 481, pp. 604-607.

[13] Lakshminarayana G., Elmahroug Y., Ashok Kumar, Dong, M.G., Dong-Eun Lee, Jonghun Yoong, Taejoon Park, 2020, TeO2–B2O3–ZnO–La2O3 glasses: γ-ray and neutron attenuation characteristics analysis by WinXCOM program, MCNP5, Geant4, and Penelope simulation codes, Ceramics International, 46, Pp16620-16635

[14] Agar O., Sayyed M.I., Tekin H.O., Kawa M. Kaky, Baki S.O., Kityk I., 2020, An investigation on shielding properties of BaO, MoO3 and P2O5 based glasses using MCNPX code, 12, pp. 629-634

[15] Yasser B. Saddeek, Shams A.M. Issa, Alharbi T., Aly K., Mahmoud Ahmad, Tekine H.O., 2020, Mechanical and nuclear shielding properties of sodium cadmium borate glasses: Impact of cadmium oxide additive, Ceramics International, 46, 2661-2669

[16] Sayyed M.I., Ashok Kumar, Tekind H.O., Ramandeep Kaur, Mandeep Singh, Agarg O., Mayeen Uddin Khandaker, 2020, Evaluation of gamma-ray and neutron shielding features of heavy metals doped Bi2O3-BaO-Na2O-MgO-B2O3 glass systems, Progress in Nuclear Energy, 118.

[17] Reza Bagheri and Ruhollah Adeli, 2020, Gamma-ray shielding properties of phosphate glasses containing Bi2O3, PbO, and BaO in different rates, Radiation Physics and Chemistry, 174, 108918

[18] Al-Buriahi M.S., Abouhaswa A.S., Tekin H.O., Sriwunkum C., El-Agawany, Nutaro F.I., T., Esra Kavaz, Rammah Y.S., 2020, Structure, optical, gamma-ray and neutron shielding properties of NiO doped B2O3–BaCO3–Li2O3 glass systems, Ceramics International, 46, pp. 1711-1721

[19] Bünyamin Aygün, Erdem Şakar, Esra Cinan, Nergiz Yıldız Yorgun, Sayyed M.I., Agare O., Abdulhalik Karabulut, 2020, Development and production of metal oxide doped glasses for gamma ray and fast neutron shielding, Radiation Physics and Chemistry, 174, 108897

[20] Agar O., Khattari Z.Y., Sayyed M.I., Tekin H.O., Al-Omari S., Maghrabi M., Zaid M.H.M., and Kityk I.V., Evaluation of the shielding parameters of alkaline earth based phosphate glasses using MCNPX code, 2019, 12, Pp. 101-106

[21] Elbashar, YH., Abd El-Ghany, HA., 2017. Optical spectroscopic analysis of Fe2O3 doped CuO containing phosphate glass. Opt. Quant. Electron. 49:310, P. 1-13.

[22] Abd El-Ghany, HA., 2018. Characterization and Optical Properties of MnO Doped CuO-Containing Phosphate Glass as Absorption Filters. J. Adv. Phys. 15, P. 5983-5996.

[23] Abd El-Ghany, HA., 2018. Development of a New Glass for Both Visible and Near-Infrared Optical Applications. Key Eng. Mater. 786, P. 224-235.

[24] Haijian Li, Jianhua Yi, Zhao Qin, Zhihua Sun, Yi Xu, Changjian Wang, Fengqi Zhao, Yucheng Hao, Xiaofeng Liang, 2019, Structures, thermal expansion, chemical stability and crystallization behavior of phosphate-based glasses by influence of rare earth, Journal of Non-Crystalline Solids, 522, 119602

[25] Grelowska, I. Roben, M. Burtan, B. Sitarz, M. Cisowski, J. Sayed, Y.E. Knapik, A. and Dodek, M., 2016, Structural and optical study of tellurite-barium glasses. Journal of Molecular structure, 1126, P. 219-225.

[26] Maiti, P.K., Mallik, A., Basumajumdar, A. and Guha, P., 2012, "Influence of barium oxide on the crystallization, microstructure and mechanical properties of potassium fluorophlogopite glass-ceramics", Journal of Ceramics International. 38, P. 251-258.

[27] Agar, O., 2018. Investigation on Gamma Radiation Shielding Behaviour of CdO–WO3– TeO2 Glasses from 0.015 to 10 MeV. Cumhuriyet Sci. J., 39, P.983-990

[28] Erdem Şakar, Özgür Fırat Özpolat, Bünyamin Alım, Sayyed M.I., Murat Kurudirek, Phy-X / PSD: Development of a user friendly online software for calculation of parameters relevant to radiation shielding and dosimetry, 2020, 166, 108496

[29] Hubbell, JH., 1982. Photon mass attenuation and energy-absorption coefficients. Int. J Appl. Radiat. Isot., 33 P.1269–1290.

[30] Sayyed M.I., Tekin H.O., ılıcoglu O. K, Agar O., Zaid M.H.M., 2018 Shielding features of concrete types containing sepiolite mineral: Comprehensive study on experimental, XCOM and MCNPX results, results in physics, 11, P.40-45

[31] Kumar, A., 2017 Gamma ray shielding properties of PbO-Li2O-B2O3 glasses. Radiat. Phys. Chem., 2017; 136:50–3.

[32] T.Z. Amer, Sara E. Saleh, R. M. El Shazly, N.S. Gomaa, A.A. Bahgat, 2019, Study of the physical and nuclear properties of liquid PbBiCd alloy coolant in nuclear fast reactor, Journal of Nuclear Materials 522, 226-235.

[33] El Shazly R. M. and Sadawy M.M., Effect of Slag as a Fine Aggregate on Mechanical, Corrosion, and Nuclear Attenuation Properties of Concrete, 2107, International Journal of Scientific Engineering and Research (IJSER), 6, 2347-3878

[34] Akman, F. Geçibesler, IH. Sayyed MI, Tijani, SA. Tufekci, AR. Demirtas, I., 2018. Determination of some useful radiation interaction parameters for waste foods. Nucl. Eng. Technol. 50, P.944–949.

[35] Sayyed MI. and Lakshminarayana, G., 2018. Structural, thermal, optical features and shielding parameters investigations of optical glasses for gamma radiation shielding and defense applications. J. Non Cryst. Solids., 487, P.53–59.

[36] Lakshminarayana, G., Baki, S.O., Lira, A., Kityk, I.V., Caldiño, U., Kaky, K.M., Mahdi, M.A., 2017. Structural, thermal and optical investigations of Dy3+-doped B2O3–WO3–ZnO–Li2O–Na2O glasses for warm white light emitting applications. J. Lumin.